

3D map of theranostic nanoparticles distribution in mice brain and liver by means of X-ray Phase Contrast Tomography

To cite this article: E. Longo *et al* 2018 *JINST* 13 C01049

View the [article online](#) for updates and enhancements.

You may also like

- [Contrast settling in cerebral aneurysm angiography](#)
Zhi-Jie Wang, Kenneth R Hoffmann, Zhou Wang et al.
- [An examination of automatic exposure control regimes for two digital radiography systems](#)
N W Marshall
- [Experimentally enhanced model-based deconvolution of propagation-based phase-contrast data](#)
M. Pichotka, K. Palma, S. Hasn et al.



ECS The Electrochemical Society
Advancing solid state & electrochemical science & technology

ECS UNITED

247th ECS Meeting
Montréal, Canada
May 18-22, 2025
Palais des Congrès de Montréal

Showcase your science!

Abstracts due December 6th

INTERNATIONAL WORKSHOP ON IMAGING II
4–8 SEPTEMBER 2017
VARENNA, ITALY

3D map of theranostic nanoparticles distribution in mice brain and liver by means of X-ray Phase Contrast Tomography

E. Longo,^a A. Bravin,^b F. Brun,^c I. Bukreeva,^c A. Cedola,^c M. Fratini,^{c,d} X. Le Guevel,^e L. Massimi,^c L. Sancey,^e O. Tillement,^f P. Zeitoun^{a,1} and O. de La Rochefoucauld^g

^aLaboratoire d'Optique Appliquée UMR7639, ENSTA-CNRS-Ecole Polytechnique-Université Paris-Saclay, 181 chemin de la Hunière et des Joncherettes, 91762 Palaiseau cedex, France

^bEuropean Synchrotron Radiation Facility, 71 Avenue de Martyrs, 38043 Grenoble cedex, France

^cInstitute of Nanotechnology-CNR, Rome-Unit, Piazzale Aldo Moro 5 00185, Rome, Italy

^dSanta Lucia Foundation, MARBLab, Via Ardeatina 306/354, 00142, Roma, Italy

^eInstitute for Advanced Biosciences U1209 UMR5309 UGA, Allée des Alpes - Site Santé, 38700 La Tronche, Grenoble, France

^fInstitut lumière-matière, UMR5306, Université Claude Bernard Lyon1-CNRS, Université de Lyon, 69622 Villeurbanne, France

^gImagine Optic, Rue François Mitterrand, 33400 Talence, France

E-mail: philippe.zeitoun@ensta-paristech.fr

ABSTRACT: The word “theranostic” derives from the fusion of two terms: therapeutic and diagnostic. It is a promising research field that aims to develop innovative therapies with high target specificity by exploiting the therapeutic and diagnostic properties, in particular for metal-based nanoparticles (NPs) developed to erase cancer.

In the framework of a combined research program on low dose X-ray imaging and theranostic nanoparticles (NPs), high resolution Phase-Contrast Tomography images of mice organs injected with gadolinium and gold-NPs were acquired at the European Synchrotron Radiation Facility (ESRF). Both compounds are good X-ray contrast agents due to their high attenuation coefficient with respect to biological tissues, especially immediately above K-edge energy. X-ray tomography is a powerful non-invasive technique to image the 3D vasculature network in order to detect abnormalities. Phase contrast methods provide more detailed anatomical information with higher discrimination among soft tissues.

¹Corresponding author.

We present the images of mice liver and brain injected with gold and gadolinium NPs, respectively. We discuss different image processing methods used aiming at enhancing the accuracy on localizing nanoparticles.

KEYWORDS: Computerized Tomography (CT) and Computed Radiography (CR); Medical-image reconstruction methods and algorithms, computer-aided diagnosis

Contents

1	Introduction	1
2	X-ray Phase Contrast Tomography (XPCT)	2
3	Results and discussion	3
3.1	Mouse brain imaging	3
3.2	Mouse liver imaging	3
3.3	3D rendering	4
4	Conclusions	4

1 Introduction

In oncology, theranostics is a modern research branch developed to optimize treatments by means of the administration of small metal based-compounds with nanometer size. The innovation introduced by theranostic nanoparticles (NPs) relies on the dual activity (therapeutic and diagnostic) exerted by these agents once they accumulate in deep tumors, such as glioblastoma, lung cancer or melanoma metastases [1, 2]. Owing to their inner core based on high Z-number metals, NPs show impressive contrast properties that allow the easy detection of tumor masses by means of imaging techniques such as X-ray tomography, MRI or PET. At the same time, thanks to their therapeutic function, they contribute to the production of free radicals to kill cancer cells during radiotherapy sessions performed few hours after their injection [3]. The development of more and more efficient NPs for theranostic use requires a rigorous study of their distribution in organs. Several microscopic imaging techniques (LIBS, dual photon microscopy, AFM) and histology sectioning have been employed for this purpose [4]. Unfortunately, if on one hand they are capable to produce high-resolution images; on the other they present a wide range of limitations. For instance, all of the mentioned techniques above imply dissecting the sample to examine the composition of its tissues, by causing an irreversible damage to the specimen and a substantial loss of information in the produced slices. In few methods, fluorescent probes are adopted with the further risk of compromising the real distribution of NPs. As consequence, the rendering of the 3D distribution of theranostic NPs becomes very complicated and challenging. In this work, we propose, for the first time, an alternative approach to trace NPs dispersions in mice organs. The images presented here were collected through high-resolution X-ray synchrotron Phase Contrast Tomography (XPCT), a technique capable to provide important 3D information about the inner structure of a specimen in a non-destructive manner. Generally, XPCT is widely used to investigate the complicated structure of microvascular or neuronal network in mice models [5–7]. Next to this well-established application, we propose the use of XPCT to detect theranostic NPs in mice samples. This employment of XPCT sounds innovative, promising and it acts as a complementary tool to other investigative

imaging protocols already used for the evaluation of the bio-distribution of NPs in mice models. This work was conceived to confirm that NPs have the capacity to accumulate in tumor areas and that a big amount of them still remain entrapped in the liver several hours after the injection. At this purpose, we present XPCT images of a mouse brain affected by melanoma metastases 1 hour after the injection of gadolinium based-NPs, named AGuIX® and, of a liver 5 hours after the administration of gold zwitterion nanoclusters, AuZwMe₂ [8]. We propose also the 3D rendering with segmentation of the entire liver volume.

2 X-ray Phase Contrast Tomography (XPCT)

XPCT allows retrieving anatomical information of soft tissues for which traditional absorption tomography gives low quality images [9–11]. The approach used in this work to access to internal microstructures of the specimen was that of the “in-line XPCT” by using X-ray parallel beam from a synchrotron light source. The in-line phase-contrast technique consists in leaving a propagation distance between the sample and the CMOS camera, in order to record the wavefront that has been distorted by the sample, thus producing an edge enhancement effect in the final reconstructed images [12–15]. The experiment was carried out at the biomedical beamline ID17 at ESRF in Grenoble, France. With the aim of better exploiting the contrast properties offered by gold and gadolinium NPs, the monochromatic incident radiation was fixed at 48.5 keV for gadolinium and 82.2 keV for gold. In both cases, the energy values were chosen in close proximity to their corresponding K-edge. At this energy, the contrast between soft tissue with poor absorption capacity and the NPs is impressive, allowing better discriminating the presence of NPs. The examined samples were a mouse brain extracted 1 hour after the injection of 15 μmol of AGuIX® NPs, NPs made of Gd and Si, and a mouse liver explanted 5 hours after the administration of 5 mg Au/mL (200 μL) of gold nanoclusters AuZwMe₂. According to the energy set for scanning the samples, the distance sample-CMOS is adjusted to satisfy the near-field condition. Therefore, the brain injected with gadolinium was placed at 2.3 m far from the CMOS whereas the liver with gold NPs at a distance of 11 m from the camera. The samples were placed in Eppendorf tubes and immobilized in agar-agar. The entire volumes of the brain and of the liver were acquired over 360° with a single-image acquisition of 0.07 s. High resolution radiographs were captured thanks to a camera pixel size of 3 μm. The collected projections were elaborated by means of the software SYRMEP Tomo Project [16]. As initial step of the data analysis, the projections were flat-field corrected. Paganin’s algorithm was used to perform the phase retrieval [17, 18] and the slices were obtained by applying the common Filtered Back Projection algorithm in combination with the Shepp-Logan filter. Some minor artifacts, such as rings and oversaturation of the central pixels produced by the rotation of the sample, were manipulated by means of the open-source software FIJI. The rings were deleted by applying Münch’s ring removal plugin [19] in polar coordinates, whereas the oversaturation in correspondence of the centre of rotation was attenuated with a band pass filter and by subtracting the background. The 3D rendering of the liver was achieved by means of the software VolView.

3 Results and discussion

3.1 Mouse brain imaging

We measured the entire mouse brain carrying several melanoma metastases by XPCT with a spatial resolution of $3\ \mu\text{m}$. In this work, we focused at presenting a specific region of the brain where nervous system, vessels and tumors doped with AGuIX® appear visible at the same time (figure 1a). The volume shown in figure 1a was imaged at 48.5 keV, just below gadolinium K-edge and its thickness is equal to $765\ \mu\text{m}$. The detailed 3D section was obtained by means of the projection of maximum intensity values of a stack of 255 slices. This 3D imaging method corresponds to project the voxels with the highest values, providing a map of the densest objects inside a sample. In the brain under investigation, the strong contrast is due to the efficient capacity of tumor targeting of AGuIX® NPs that were able to reach many metastases (big white masses indicated by red arrows) located in different regions of the brain. It appears that a little concentration of NPs was even entrapped in small vessels.

3.2 Mouse liver imaging

The entire mouse liver doped with gold NPs was imaged at 82.20 keV, above gold K-edge, with the aim of better distinguishing the gold NPs in respect from the soft tissue (figure 1b). Thanks to the high resolution ($3\ \mu\text{m}$) and to the phase contrast technique, the full anatomy of the liver is displayed with impressive sensitivity, but the detection of gold NPs 5 hours after their injection revealed to be complicated. From the fully reconstructed dataset, it seems that gold NPs scattered everywhere in the soft tissue without forming clusters large enough to be immediately recognized with XPCT. However, distinct white areas made up of very small spots alternate to shady regions, giving a promising idea that it could be the signal attributable to the presence of gold NPs.

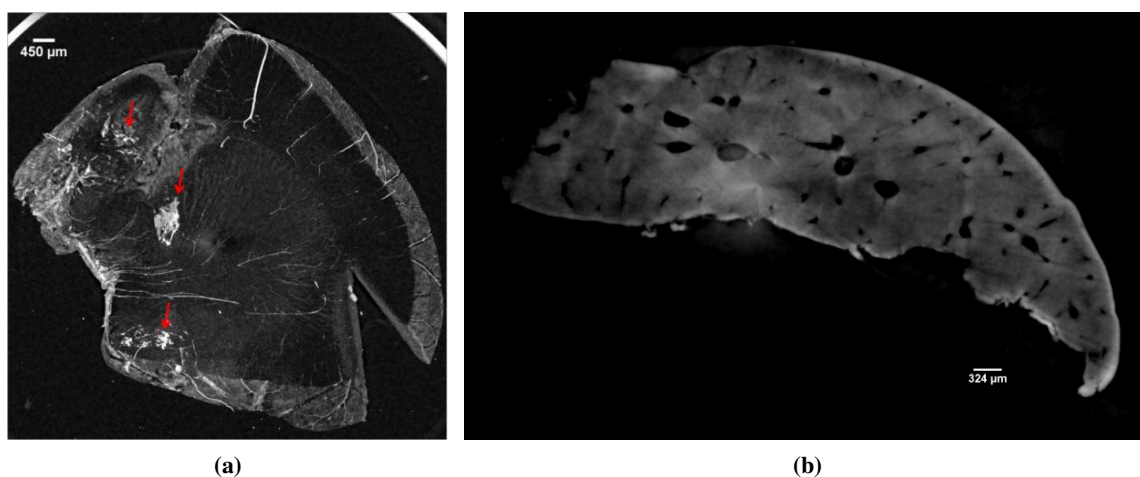


Figure 1. (a) On the left, Maximum Intensities Projection (MIP) of a $765\ \mu\text{m}$ thickness of the mouse brain. Sample courtesy of [1]. The image shows the presence of AGuIX® NPs in tumor areas and in few vessels. (b) Reconstructed slice representing the coronal section of the mouse liver. Gold NPs reached the liver without aggregating in larger clusters. They are scattered everywhere in the tissue and this makes their localization more difficult. However, their weak signal could be associated to numerous small bright spots present in the image, and in greater contribution around the hepatic vessels.

3.3 3D rendering

XPCT allows reproducing the full sample volume owing to the multiple views acquired under many angles. In this paper, we display the 3D rendering of the entire liver obtained through the use of the open-source software VolView (figure 2). The software is conceived to realize the segmentation of a sample by establishing a transfer function between the gray level of the image representing different anatomic characteristics and a color map. The final 3D model of the liver shows in yellow color a bright patina around the skin of the liver. Since this yellow skin is related to the highest intensity values, it could be the signature of the scattered signal produced by gold NPs deposited on the external side of the liver or, it could be the consequence of a phase retrieval not optimally tuned because of the complicated chemical composition of the sample. Data treatment is still under progress to confirm the gold NPs localization.

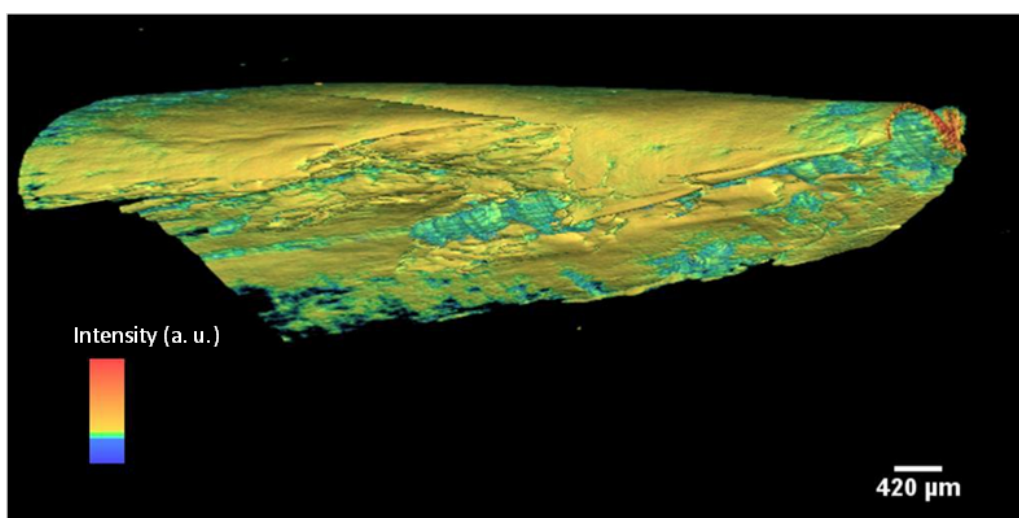


Figure 2. 3D false color rendering of a mouse liver. The presence of gold NPs seems to concentrate on the liver outer part (yellow), where also the XPCT artificial signal enhancement is the highest. Data treatment is still under progress to confirm the localization of gold NPs.

4 Conclusions

Thanks to the high power of targeting and accumulation of AGuIX® NPs in tumors, XPCT has proven to be an efficient method in identifying the accurate location of the tumors in the brain and in imaging them at high spatial resolutions. A little concentration of AGuIX® NPs was also observed in blood vessels according to the AGuIX® kinetics of distribution, whereby the half-life time of these NPs in blood is 21.6 min [4]. To what concern the imaging of the retention of gold NPs in the liver, the results appear more complicated to be interpreted with the only XPCT method. It seems that gold NPs diffused everywhere in the tissue by producing a scattered signal all over the liver, therefore the technique adopted does not allow for accurate discrimination between NPs and tissue. However, XPCT earned a chance to be considered as a complementary method to study the biodistribution of NPs in mice samples, by allowing their 3D reconstruction in a non-destructive manner.

Acknowledgments

This work was partially funded by the VOXEL project (European Union's Horizon 2020 research and innovation program under grant agreement N° 665207) and COST Action MP1203.

References

- [1] S. Kotb et al., *Gadolinium-Based Nanoparticles and Radiation Therapy for Multiple Brain Melanoma Metastases: Proof of Concept before Phase I Trial*, *Theranostics* **6** (2016) 418.
- [2] S. Dufort et al., *Nebulized gadolinium-based nanoparticles: A theranostic approach for lung tumor imaging and radiosensitization*, *Small* **11** (2015) 215.
- [3] L. Sancey et al., *The use of theranostic gadolinium-based nanoprobess to improve radiotherapy efficacy*, *Br. J. Radiol.* **87** (2014) 20140134.
- [4] L. Sancey et al., *Long-term in Vivo clearance of gadolinium-based AGuIX nanoparticles and their biocompatibility after systemic injection*, *ACS Nano* **9** (2015) 2477.
- [5] M. Fratini et al., *Simultaneous submicrometric 3D imaging of the micro-vascular network and the neuronal system in a mouse spinal cord*, *Sci. Rept.* **5** (2015) 8514.
- [6] A. Cedola et al., *X-Ray Phase Contrast Tomography Reveals Early Vascular Alterations and Neuronal Loss in a Multiple Sclerosis Model*, *Sci. Rept.* **7** (2017) 1.
- [7] I. Bukreeva et al., *Quantitative 3D investigation of Neuronal network in mouse spinal cord model*, *Sci. Rept.* **7** (2017) 41054.
- [8] D. Shen et al., *Zwitterion functionalized gold nanoclusters for multimodal near infrared fluorescence and photoacoustic imaging*, *APL Mater.* **5** (2017) 053404.
- [9] C.A. Carlsson, *Imaging modalities in x-ray computerized tomography and in selected volume tomography*, *Phys. Med. Biol.* **44** (1999) R23.
- [10] T. Weitkamp et al., *X-ray phase imaging with a grating interferometer*, *Opt. Express* **13** (2005) 6296.
- [11] A. Bravin, P. Coan and P. Suortti, *X-ray phase-contrast imaging: From pre-clinical applications towards clinics*, *Phys. Med. Biol.* **58** (2013) R1.
- [12] A. Snigirev, I. Snigireva, V. Kohn, S. Kuznetsov and I. Schelokov, *On the possibilities of x-ray phase contrast by coherent high-energy synchrotron radiation*, *Rev. Sci. Instrum.* **66** (1995) 5486.
- [13] S.W. Wilkins, T.E. Gureyev, D. Gao, A. Pogany and A.W. Stevenson, *Phase-contrast imaging using polychromatic hard x-rays*, *Nature* **384** (1996) 335.
- [14] R. Fitzgerald, *Phase-sensitive X-ray imaging*, *Phys. Today* **53** (2000) 23.
- [15] T. Weitkamp, D. Haas, D. Wegrzynek and A. Rack, *ANKAphase: Software for single-distance phase retrieval from inline X-ray phase-contrast radiographs*, *J. Synchrotron Radiat.* **18** (2011) 617.
- [16] F. Brun et al., *SYRMEP Tomo Project: a graphical user interface for customizing CT reconstruction workflows*, *Adv. Struct. Chem. Imaging* **3** (2017) 4.
- [17] D. Paganin, S.C. Mayo, T.E. Gureyev, P.R. Miller and S.W. Wilkins, *Simultaneous phase and amplitude extraction from a single defocused image of a homogeneous object*, *J. Microsc.* **206** (2002) 33.
- [18] M.R. Teague, *Deterministic phase retrieval: a Green's function solution*, *J. Opt. Soc. Am.* **73** (1983) 1434.
- [19] B. Münch, P. Trtik, F. Marone and M. Stampanoni, *Stripe and ring artifact removal with combined wavelet — Fourier filtering*, *Opt. Express* **17** (2009) 8567.